Dynamic PET image denoising

P. Gonzalez*, B. Alcaino*, R. Barrientos*, M. Mora*, F. Tirado* and C. Tauber+

* DCI Universidad Católica del Maule, Talca, Chile
+ UMRS INSERM U930, Université François Rabelais, Tours, France

Keywords: Dynamic PET images, Spatio-temporal filtering.

Abstract

Dynamic Positron Emission Tomography (dPET) images are inherently affected by noise and low spatial resolution. The problems aforementioned may lead to incorrect estimation of the uptake of the tracer in tissues. In this work, we present a novel method for enhancing the signal-to-noise ratio of dPET images. The method consist in a edge preserving filter based upon an indirect image. The indirect image give orientation to the treatment so as to process all frames at the same fashion. We exploit the spatial and temporal information along the entire sequence in order to adapt the filtering process to preserve edges between functional regions. Comparative experimentations on realistic simulations validate the potential of the proposed method.

1 Introduction

Dynamic Positron Emission Tomography (dPET) is used to produce maps in vivo of radio tracer distribution along the time. However, dPET images suffer from noise (low signal to noise ratio SNR) and low spatial resolution that lead to smoothed boundaries between adjacent kinetic regions. Isotropic smoothing methods such as Gaussian filtering can increase SNR but in decrement of resolution, hampering the localization of tissues for segmentation or quantification purposes. Demirkaya [1] applies an anisotropic filter based on partial differential equations for full body static PET studies. The author, combine the diffusion equation proposed by Perona and Malik [2], and the diffusion coefficients proposed by Weickert on [3], maintaining the median intensities on ROIs where the edges are defined, reducing the statistic variations without spurious artifacts. In a framework for gradient-based segmentation of PET images, Geets et al [4] proposed a variant of the bilateral filter of Tomasi and Manduchi [5], preceded by a deconvolution process using the Richardson-Lucy or Reblurred Van Cittert deconvolution method. An edge preserving denoising approach that exploits the spatio and temporal information of dPET was proposed in [6]. The method use the bilateral filter framework proposed by Tomasi and Manduchi in [5], but the weights are calculated by exploting the boxel-wise kinetic information and similarity between time-activity curves. The method reduce statitical variations while edges of kinetics regions are preserved reducing bias. Christian et al. [7], proposed a highly constrained back-projection technique to benefit from a time-averaged additional image to filter each frame. The method is a weighted convolution process in each frame. This approach increase SNR while preserving the spatial resolution of the Dynamic study.

In this work, we propose an indirect filtering for dPET image restoration. The proposed method exploits the spatial and temporal information of the tracer based on a indirect composite image. The composite image represent the entire summed dPET along the time. The method, reduces noise inside functional regions preserving the boundary between them.

To assess the performance of the proposed method, we use realistic simulations with known ground truth in order to establish an objective comparison with other edge preserving dPET restoration method.

The remainder of the paper is organized as follows. We present the proposed approach in section 2. Section 3 details the experimental setup to assess and compare the proposed filter. Results are presented in section 4 and a general conclusion is given in section 5.

2 Proposed method

In the continuous domain, a 3D vector-valued image is represented by a mapping $\mathbf{I} : \mathbb{R}^3 \rightarrow \mathbb{R}^N$, where N is the number of frames. Let $\mathbf{x} = (x_1, x_2, x_3) \in \mathbb{R}^3$, $I(\mathbf{x}, f)$ represent the value of a voxel on the spatial position $\mathbf{x}$ at f^{th} frame.

Inpired on the framework proposed by He in [8] and the composite image proposed by Christian et al. [7], given a noisy image $\mathbf{I}$, each voxel $I^F(\mathbf{x}, f)$ is calculated as follows:

$$I^F(\mathbf{x}, f) = \frac{1}{\#\omega} \sum_{k \in \omega_{\mathbf{x}}} (a_k(\mathbf{x}, f) Ic(\mathbf{x}) + b_k(\mathbf{x}, f)), \quad (1)$$

where $\omega_{\mathbf{x}}$ is the neighborhood centered on the voxel $\mathbf{x}$,

$$a_k(\mathbf{x}, f) = \frac{1}{\sigma_k^2 + \epsilon} \left(\frac{1}{\#\omega} \sum_{\mathbf{y} \in \omega_k} Ic(\mathbf{y}) I(\mathbf{y}, f) - \left(\frac{1}{\#\omega} \sum_{\mathbf{z} \in \omega_k} Ic(\mathbf{z}) \right) \left(\frac{1}{\#\omega} \sum_{\mathbf{z} \in \omega_k} I(\mathbf{z}, f) \right) \right) \quad (2)$$

and

$$b_k(\mathbf{x}, f) = \left(\frac{1}{\#\omega}\sum_{\mathbf{z}\in\omega_k} I(\mathbf{z}, f)\right) - a_k(\mathbf{x}, f)\left(\frac{1}{\#\omega}\sum_{\mathbf{z}\in\omega_k} Ic(\mathbf{z})\right). \quad (3)$$

The composite image Ic, is calculated at the same way as proposed by Christian et al. in [7]. Edge preservation is given by the linear coefficients. Considering the variance σ_k^2 and the regularization parameter ϵ, boundering regions are defined according to variability on the regions of interest. Considering a $\epsilon > 0$ value, two cases can be defined:

- $\sigma_k^2 \gg \epsilon$: contour region. Therefore, $a_k \approx 1$ and $b_k \approx 0$.
- $\sigma_k^2 \ll \epsilon$: homogeneous region. In this case, $a_k \approx 0$ and $b_k \approx \mu_k$.

where μ_k is the mean of Ic in ω_k

3 Experimentations

3.1 Simulated images

In our experimentations, we used realistics analytical simulations of dynamic brain PET images proposed in [9]. The simulated images were obtained from a hight resolution numerical phantom with labeled ROIs using TACs extracted from real acquisitions with a beta-emitter 11C-PE2I. The simulations are based on an analytic ASIM approach, extended as follows:

- Partial volume effect modelization.
- Projection model based on real crystal coordinates.
- Fam-sum based random distribution.
- An intrinsic modeling of the decay and count rates through the dynamic acquisition.

3.2 Comparison to another method

- HighlY constrained backPRojection (HYPR): Proposed by Christian et al in [7], exploit the hight SNR of the time-averaged composite image used to weight a convolution process in each frame. HYPR is calculated as follows:

$$I_f^{Hypr} = Ic\frac{K \otimes I_f}{K \otimes Ic}, \quad (4)$$

where K is a gaussian kernel, $\otimes$ denotes the convolution operator and I_f is the frame of the noisy image. The composite volume is calculated as follows:

$$Ic = \sum_f I_f \cdot \Delta t_f \quad (5)$$

where Δt_f is the time duration (acquisition time) of each frame f.

3.3 Quantitative criteria

The following quantitative criteria were measured:

- Signal to Noise Ratio (SNR) was defined as:

$$10log_{10}\left(\frac{||I^{truth}||}{||I^{truth} - I^{res}||}\right)^2, \quad (6)$$

where I^{truth} is the ground truth and I^{res} the image resulting from the filtering process.

- Bias(BIAS) was defined as:

$$BIAS = \frac{1}{R}\frac{1}{M}\sum_{i=1}^{R}\sum_{m=1}^{M}|RC_{i,m} - 1|, \quad (7)$$

where R is the number of regions and M the number of frames. A quantitative criteria traditionally used in statistical PET imaging is called recovery coefficients ($RC_{i,m}$). These coefficients measure the ratio of $\overline{R}_{i,m}$, which denotes the average activity concentration observed in a region R_i in the frame I_m and the actual activity $R^*_{i,m}$ of the same region and same frame, obtained on the ground truth. The overall bias scores is always positive. It takes into account simultaneously all regions and all frames of the dynamic PET image.

- Mean Square Error (MSE) was defined as:

$$MSE = \left(\frac{1}{R}\frac{1}{M}\sum_{i=1}^{R}\sum_{m=1}^{M}\left|\frac{\overline{R}_{i,m} - R^*_{i,m}}{R^*_{i,m}}\right|\right)^2 + \frac{1}{R}\frac{1}{M}\sum_{i=1}^{R}\sum_{m=1}^{M}\left(\frac{R_{i,m} - \overline{R}_{i,m}}{R^*_{i,m}}\right)^2, \quad (8)$$

where $\overline{R}_{i,m}$ denotes the averaged activity concentration observed in the region R_i on the frame I_m, $R^*_{i,m}$ is the real concentration in the region i on frame m. Finally, R and M correspond with the number of regions and frames respectively.

- Adjusted Rand Index (ARI) was defined by:

$$\frac{index - expected\ index}{max\ index - expected\ index}. \quad (9)$$

ARI is a similarity measure between a classification result and the ideal classification. ARI return a value between 0 and 1. The value increase with the segmentation quality.

4 Results

4.1 Visual results

To validate the proposed method, realistic simulations defined in section 3.1 were carried out. We compared the unprocessed simulated image (UI) with HYPR and the proposed method.

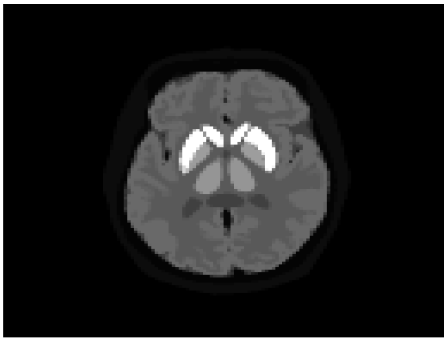

(a)

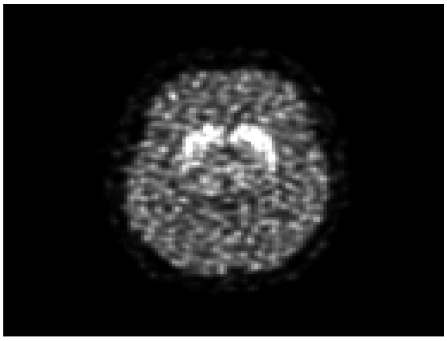

(b)

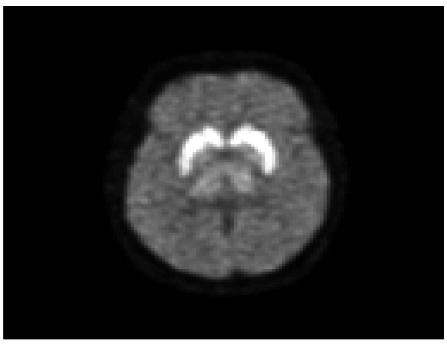

(c)

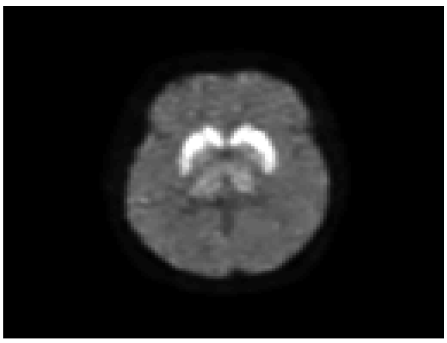

(d)

Figure 1. Sample view of the 12th frame, axial slice obtained for HYPR and proposed method applied on simulated images with 50 iterations during reconstruction: (a) Ground truth, (b) Unprocessed image, (c) HYPR, and (d) Proposed method.

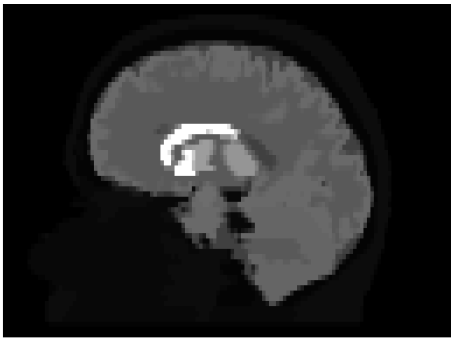

(a)

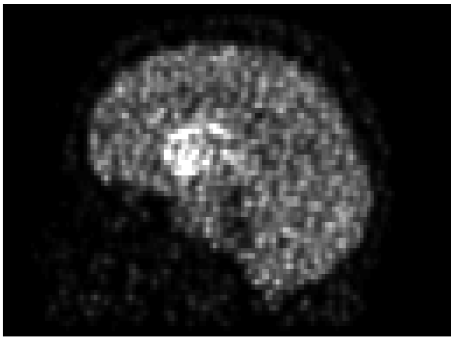

(b)

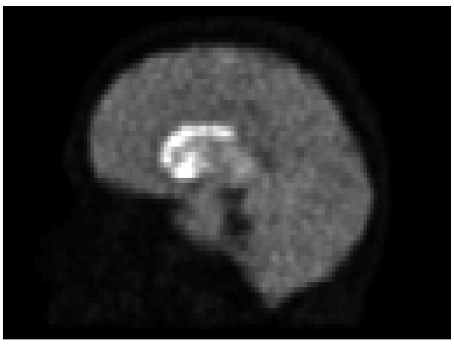

(c)

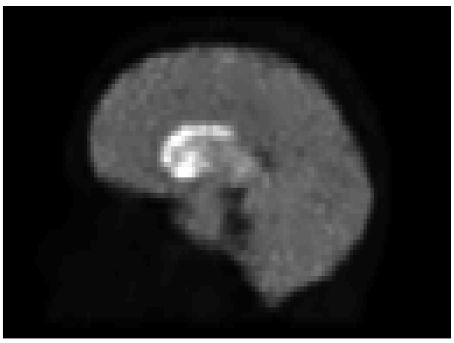

(d)

Figure 2. Sample view of the 12th frame, sagittal slice obtained for HYPR and proposed method applied on simulated images with 50 iterations during reconstruction: (a) Ground truth, (b) Unprocessed image, (c) HYPR, and (d) Proposed method.

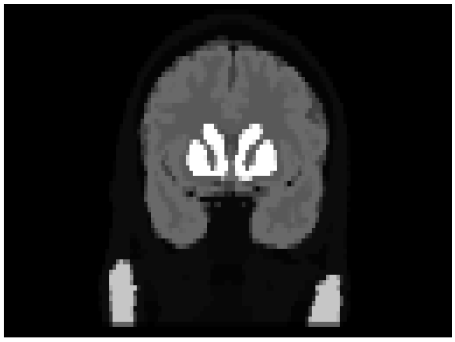

(a)

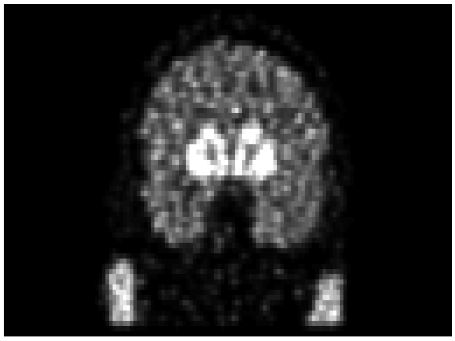

(b)

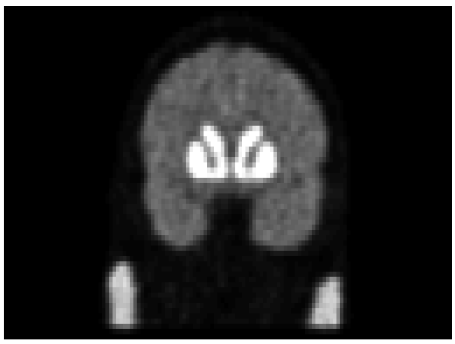

(c)

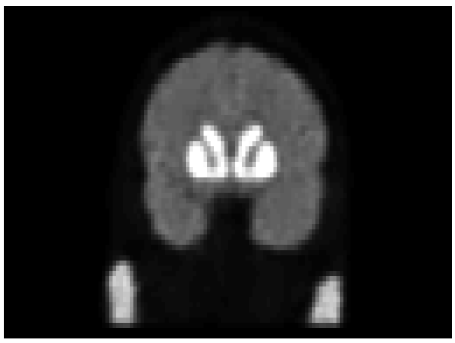

(d)

Figure 3. Sample view of the 12th frame, coronal slice obtained for HYPR and proposed method applied on simulated images with 50 iterations during reconstruction: (a) Ground truth, (b) Unprocessed image, (c) HYPR, and (d) Proposed method.

Representative results are displayed in figures 1, 2 and 3, where the noise reduction and edge preservation of the proposed method can be observed compared to HYPR. Figures 1(c) and 1(d) shows representative results of 12th frame on the axial slice. Figures 2(c) and 2(d) shows representative results of 12th frame on the sagittal slice. Figures 3(c) and 3(d) shows representative results of 12th frame on the coronal slice. A visual inspection suggest that the two methods can preserve spatial resolution but the proposed method produce more effective denoise than HYPR.

4.2 Quantitative results

Quantitative assessment of the results are shown in figures 4, 5, 6, 7 and table 1. Objective results were achieved by using the criterias presented in the section 3.3. Values were obtained in comparison the resultant dynamic volumes of the methods with the ground truth.

We separate the results that present quality of the resulting dynamic volume and as a previous stage to a segmentation process.

Graphics of figures 4, 5 and 6 show the results calculated from 1280 volumes (64 dynamic simulations) by using TSNR, BIAS and ECM criterias.

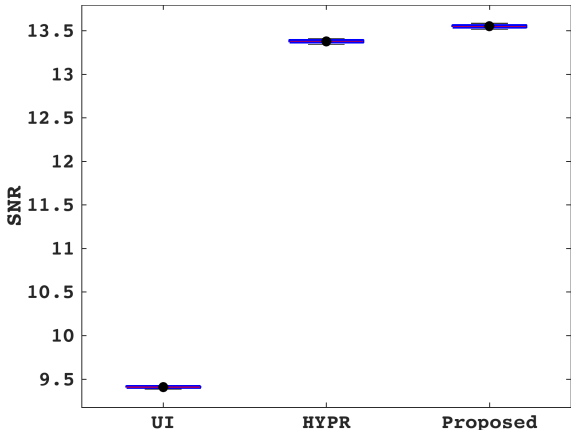

Figure 4. TSNR quantitative criteria for quality of the filter process on 64 realistic volume simulations.

Graphic of the figure 7 show the quality of segmentation, measured by using the ARI criteria. The k-means algorithm was used for each filtered dynamic volume and compared with the ideal segmentation of the ground truth. Higher value of ARI indicate a better quality of the segmentation process.

Method	SNR	BIAS	MSE	ARI
UI	9.41 ± 0.01	0.2615 ± 0.009	1.62 ± 0.06	0.27 ± 0.002
HYPR	13.38 ± 0.02	0.2888 ± 0.006	0.74 ± 0.02	0.26 ± 0.005
WCGF	$\mathbf{13.55 \pm 0.02}$	$\mathbf{0.2876 \pm 0.007}$	$\mathbf{0.69 \pm 0.02}$	$\mathbf{0.28 \pm 0.003}$

Table 1. Figures of merit averaged over 64 simulations.

Average values obtained for the performance criteria

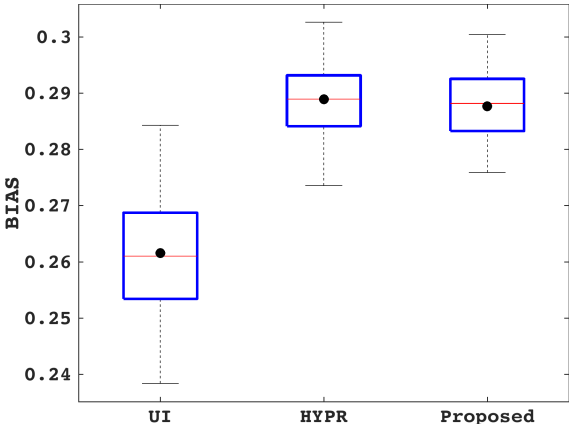

Figure 5. BIAS quantitative criteria for quality of the filter process on 64 realistic volume simulations.

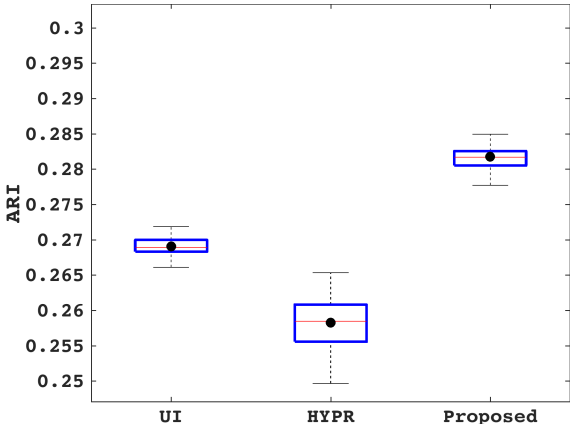

Figure 7. ARI calculated for 64 realistic volume simulations

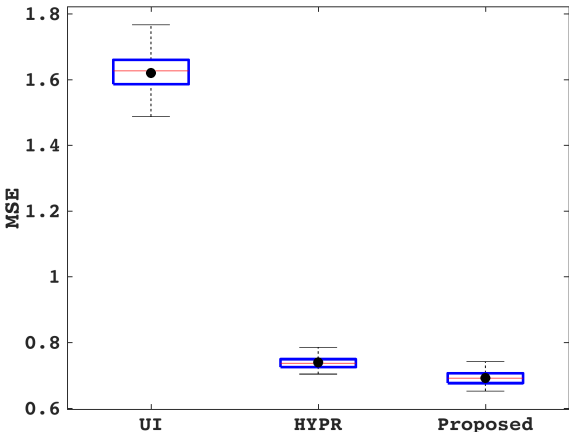

Figure 6. ECM quantitative criteria for quality of the filter process on 64 realistic volume simulations.

TSNR, shows that the improvement of this indicator has been a factor of 1.42 and 1.44 for HYPR and the proposed method respectively. The performance achieved by the methods for the criteria MSE has from 1.62 to 0.74 and 0.69 for HYPR and the proposed method respectively. Initial bias score of the unprocessed image is 0.2615, and increased to 0.2888 and 0.2876 by HYPR and the proposed method respectively.

5 Conclusion

We have proposed a method to restore dPET images. Our approach provide an alternative among filters that take profit of the consistency of the acquisition along time in order to increase de SNR in dPET. This information provides our filter with the capability of denoise all frames at the same fashion by exploiting the weighted composite image. The method reduce noise in identified homogeneous regions while preserve edges using the coefficients calculated between each frame and the composite image. In our experiments, we evaluate the quality of the dynamic volumes obtained and the behaviour of the methods as a previous stage of segmentation process. The proposed method led to improve the performance of criterias with respect of the denoising and spatial resolution preserving capability compared to HYPR. Less MSE and similar BIAS scores of the proposed method compared with HYPR, indicates better statistic variation decrease. Both methods increase proportionally the BIAS score inside ROIs, but the proposed method increase the value in a lesser extent than HYPR. Therefore, the proposed method improves the signal-to-noise ratio while maintains the spatial resolution. The ARI criteria obtained by the proposed method, confirm that facilitate the future extraction processes. In other hands, HYPR difficult the segmentation leading to errors on the quantification process.

Acknowledgment

The authors would like to thank the Laboratory of Technological Research on Pattern Recognition (www.litrp.cl), Universidad Católica del Maule, for providing the High Performance Computing servers with which the experiments were carried out.

References

[1] O. Demirkaya, "Post-reconstruction filtering of positron emission tomography whole-body emission images and attenuation maps using nonlinear diffusion filtering," *Academic radiology*, vol. 11, no. 10, pp. 1105–1114, 2004.

[2] P. Perona and J. Malik, "Scale-space and edge detection using anisotropic diffusion," *IEEE Transactions on pattern analysis and machine intelligence*, vol. 12, no. 7, pp. 629–639, 1990.

[3] J. Weickert, *Anisotropic diffusion in image processing*, vol. 1. Teubner Stuttgart, 1998.

[4] X. Geets, J. A. Lee, A. Bol, M. Lonneux, and V. Grégoire, "A gradient-based method for segmenting fdg-pet images: methodology and validation," *European journal of nuclear*

medicine and molecular imaging, vol. 34, no. 9, pp. 1427–1438, 2007.

[5] C. Tomasi and R. Manduchi, "Bilateral filtering for gray and color images," in *Computer Vision, 1998. Sixth International Conference on*, pp. 839–846, IEEE, 1998.

[6] Z. Bian, J. Huang, J. Ma, L. Lu, S. Niu, D. Zeng, Q. Feng, and W. Chen, "Dynamic positron emission tomography image restoration via a kinetics-induced bilateral filter," *PloS one*, vol. 9, no. 2, p. e89282, 2014.

[7] B. T. Christian, N. T. Vandehey, J. M. Floberg, and C. A. Mistretta, "Dynamic pet denoising with hypr processing," *Journal of Nuclear Medicine*, vol. 51, no. 7, pp. 1147–1154, 2010.

[8] K. He, J. Sun, and X. Tang, "Guided image filtering," *IEEE transactions on pattern analysis and machine intelligence*, vol. 35, no. 6, pp. 1397–1409, 2013.

[9] S. Stute, C. Tauber, C. Leroy, M. Bottlaender, V. Brulon, and C. Comtat, "Analytical simulations of dynamic pet scans with realistic count rates properties," in *Nuclear Science Symposium and Medical Imaging Conference (NSS/MIC), 2015 IEEE*, pp. 1–3, IEEE, 2015.